COMPDYN 2019
7th ECCOMAS Thematic Conference on
Computational Methods in Structural Dynamics and Earthquake Engineering
M. Papadrakakis, M. Fragiadakis (eds.)
Crete, Greece, 24–26 June 2019

CONSTANT-DUCTILITY RESIDUAL DISPLACEMENT RATIOS

M. Orlacchio[1], G. Baltzopoulos[1], and I. Iervolino[1]

[1]Università degli Studi di Napoli Federico II
Via Claudio 21, 80125 Naples, Italy
e-mail: {mabel.orlacchio, georgios.baltzopoulos, iunio.iervolino}@unina.it

Abstract

This paper presents a predictive model for evaluating the central tendency and related record-to-record variability for the residual displacements of simple inelastic oscillators under seismic excitation. For this study, yielding single-degree-of-freedom systems were considered, with bilinear backbones and non-degrading hysteretic rule characterized by peak-oriented reloading stiffness. Systems with natural periods belonging to the 0.3 s to 2.0 s range and exhibiting post-yield hardening ratios ranging from 0 to 10%, were analyzed via incremental dynamic analysis to obtain the residual displacements as a function of the ductility demand. A set of fifty acceleration records was used for the dynamic analysis, coming from medium-to-large magnitude events, recorded at the closest distance to the rupture surface ranging from 3.5 km to 43.7 km on firm soil or rock and devoid of apparent directivity effects of interest for seismic response. The model fitted on these results, consists of two regression equations: one equation for the period elongation given ductility demand and another for the residual displacement ratio given period elongation and ductility demand.
In this context, the residual displacement ratio is defined as residual-to-peak inelastic displacement. Thus, the model allows to assess the joint conditional distribution of period elongation and residual displacement at fixed ductility levels. These results could be useful for seismic reliability assessment for structures accumulating damage, for example during seismic sequences, where the seismic fragility of a structure damaged during a mainshock earthquake comes into play for risk calculations during the ensuing aftershock sequence.

Keywords: residual displacements; sequence-based seismic reliability; state-dependent seismic fragility.

1 INTRODUCTION

Within the Performance-Based Earthquake Engineering (PBEE; [1]) paradigm, the probabilistic assessment of a structure's residual displacement is of interest, in addition to the peak (transient) deformation demand, because the former can be useful in modelling the performance of structures during a seismic sequence, when these structures have been already damaged by the mainshock earthquake. In fact, the residual displacement is a response parameter closely related with the remaining capacity of mainshock-damaged structures to withstand aftershock sequences [2,3]. In this context, the residual deformation was established over the last years as a useful index of the severity of inelastic response, complementary to maximum transient response. Moreover, its amplitude can be used to determine the technical and economic feasibility of repairing seismic damages because of the difficulty to reverse permanent displacements [4]. Thus, several previous studies were focused on individuating the parameters that primarily affect residual displacement, and a few investigations also presented simple predictive equations for residual displacements.

Some early observations about residual displacement demands were provided by Mahin and Bertero [5] who found that the permanent displacements of elastoplastic systems averaged more than forty-percent of the peak inelastic displacement demand with high level of variability (coefficients of variation associated with residual displacements close to unity).

An early residual displacement predictive procedure was provided by MacRae and Kawashima [6]. They studied residual deformation demands of bilinear single-degree-of-freedom (SDOF) systems with several values of post-yield stiffness ratio, under three ductility demands. They pointed out the influence of post-yield stiffness ratio on the amplitude of residual displacements introducing a method for estimating the average value of residual displacements only dependent on the post-yield hardening ratio and the ductility demand, without identifying a clear trend with the structural period of natural vibration. Moreover, they proposed residual displacement response spectra for bilinear oscillators with varying post-yield hardening ratio [7]. The dependence of residual displacements amplitude on ductility demand and mainly on post yielding stiffness was also confirmed by Borzi et al. [8].

Subsequently, Pampanin et al. [9] studied residual displacements normalized by peak inelastic displacement demand of four equivalent SDOF systems representative of reinforced concrete (RC) frame buildings. They considered three hysteretic models (evolutionary and non-evolutionary) and different post-yielding stiffness ratios. These authors observed that the residual deformation demand depended on the type of hysteresis, seismic intensity and post-yield stiffness ratio.

Ruiz-Garcia and Miranda [4,10] studied the influence of several factors on the residual displacement ratio C_r, which they defined as the ratio of residual-to-maximum elastic displacement. These factors included period of natural vibration, lateral strength ratio, site conditions, earthquake magnitude, distance to the source, post-yield stiffness ratio and unloading stiffness. In that investigation residual displacement ratios were computed for elastoplastic, bilinear SDOF systems with kinematic strain hardening and for SDOF systems with three stiffness-degrading hysteretic models. They observed C_r to strongly depend on the lateral strength and on period of natural vibrations mainly for periods shorter than about 1.0 s. They also highlighted that residual displacements ratios exhibit record-to-record variability that should also be accounted for. Moreover, a simplified equation to estimate the central tendency of residual displacement demands for elastoplastic systems was suggested in [4], as function of two independent variables, period of natural vibration and strength ratio.

A detailed study about the influence of the hysteretic law on residual displacements was performed by Liossatou and Fardis [11]. They used hysteretic models which represent the cyclic degradation of stiffness and strength that is typical of RC structures. The scatter in residual displacements was also quantified providing at different periods of natural vibration.

The objective of this study is to present a predictive model for the central tendency and related record-to-record variability of residual displacements for SDOF bilinear systems with non-degrading hysteretic rule, characterized by peak-oriented reloading stiffness. To this end, the constant-ductility residual displacement ratio is investigated, defined as the absolute value of the ratio of residual to peak transient displacement, $C_\mu = \left|\delta_{res}/\delta_{\max}\right|$, where δ_{res} and $\delta_{\max}$ preserve their sign. This ratio is calculated for various combinations of input motion, natural vibration period and post-yielding hardening ratio. In all cases, ductility demand μ (defined as the ratio of maximum response to yield displacement of the intact system, $\mu = \delta_{\max}/\delta_y$) is held constant by appropriately scaling the input motion. Because it is typical to define the damage state of a structure based on crossing maximum transient displacement thresholds (e.g., [12,13]), this constant-ductility approach could be useful in the context of simplified estimation of state-dependent seismic fragility [2,3,14]. The main result of the study is a predictive equation for C_μ, derived via two-stage regression [15].

The article is structured as follows: first the analysis methodology is outlined describing the properties of the analyzed systems and the organization of the analyses used to collect the data set. The next two sections are dedicated to the detailed description of the predictive model development, presenting first the model for residual displacement and secondly the model for period elongation. Finally, the evaluation of the predictive model effectiveness is presented along with some evaluation and discussion of the obtained results.

2. ANALYSIS METHODOLOGY

In order to collect the required data on which to base the predictive model, yielding single-degree-of-freedom systems with bilinear backbone and modified Ibarra-Medina-Krawinkler (IMK) hysteretic model [16] were analyzed. Figure 1a shows an example of bilinear backbone and hysteresis in dimensionless $\{R, \mu\}$ coordinates, where $R = Sa(T)/Sa(T)_y$ is the strength ratio, defined as the ratio of spectral acceleration intensity to its value causing yield or, equivalently, the ratio of the elastic force over the yield base shear of the system, and μ is the ductility demand. The backbone starts elastically and presents a following hardening segment with a slope α_h, representing the ratio of post-yield stiffness to elastic stiffness, which ends at the capping point ductility μ_c where the loss of strength begins. Figure 1a reports a descending branch too, defined by the post-capping slope α_c, the ratio of the negative post-capping stiffness to elastic stiffness, and the fracture ductility, μ_f, point corresponding to complete loss of strength. This latter branch was defined exclusively for keeping track of the capping points in the damaged post-shock state, whilst only considering target ductility demands lower than the capping ductility during the execution of nonlinear dynamic time-history analyses. Figure 1b shows the modified IMK hysteretic model with peak-oriented response (presented in detail in [17]). This hysteretic model is characterized by peak-oriented reloading stiffness; therefore, the direction of the loading path targets the maximum displacement on the opposite side once the horizontal axis is intersected in each reloading cycle. Although the model can include cyclic deterioration modes, in this study it was implemented without considering any degradation rules for strength and unloading stiffness.

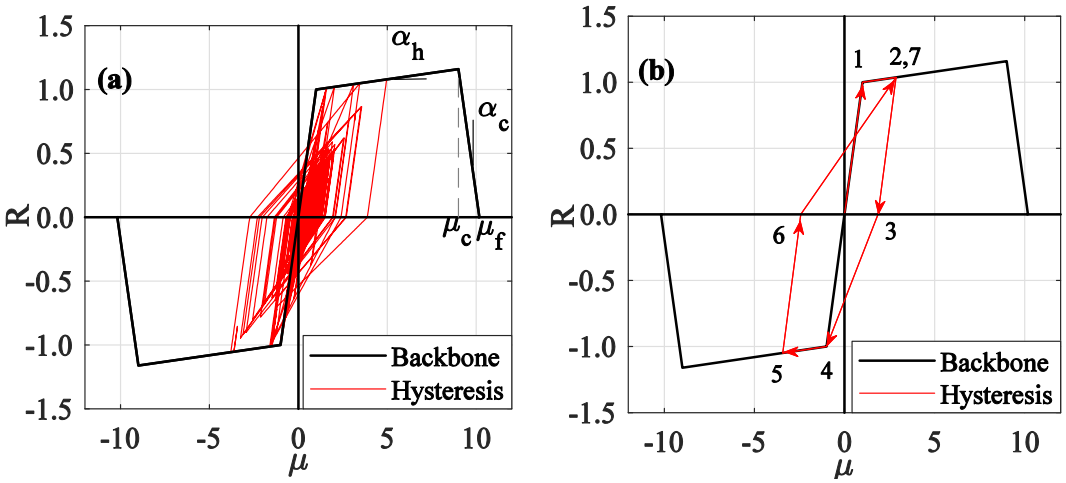

Figure 1: Backbone curve and non-degrading Modified Ibarra Medina Krawinkler (IMK) peak-oriented hysteretic model in dimensionless $\{R, \mu\}$ coordinates: backbone curve with defining parameters and an example of hysteresis for the case with $T = 1.0s$, $\alpha_h = 2.0\%$ and $\mu = 5.0$ (**a**); representation of IMK hysteretic model with peak-oriented response (**b**).

The residual displacements of the SDOF systems were computed using a set of analyses organized in two different phases. The first phase consists in the execution of *incremental dynamic analysis* (IDA) [18] fixing the target ductility μ, which defines the damage state reached by the structure during the earthquake. In this phase, the SDOFs are subjected to a suite of fifty earthquake ground motions selected from within the NESS dataset [19]. These ground motions were recorded on firm soil at a closest distance to the rupture surface (R_{RUP}) ranging from 3.5 km to 43.7 km and coming from seismic events with moment magnitude belonging to the 6.1-7.6 range. Furthermore, the selected records exhibit PGA ranging from 0.053 g to 1.43 g and are devoid of apparent directivity effects. IDA involves performing a set of nonlinear dynamic analyses using each record scaled in amplitude to increasing levels of intensity, represented by an intensity measure (IM), to reach or pass the limit of engineering demand parameter (EDP), the structural response corresponding to the level of ductility demand for each damage state. Thereby a scale factor (SF) for each accelerogram is evaluated to bring the response of the structural model to a fixed damaging level. The second phase consists in obtaining multiple realizations of the SDOF structure in post-mainshock damage state by performing non-linear dynamic analysis, using the records scaled by the SF calculated in the previous phase. Subsequently a *static pushover analysis* up to the collapse is performed for each realization, in both positive and negative direction of the load.

The performed analyses differ in the assumed values of ductility demand μ, period of natural vibration T and post-yield hardening ratios α_h of SDOF systems. Ductility demand assumed the following values $\mu = \{1.5, 2.0, 3.0, 4.0, 5.0, 6.0, 7.0, 8.0, 9.0\}$. The analyzed oscillators had a fixed backbone as shown in Figure 1. In detail, the bilinear backbone was defined assuming period, in seconds, $T = \{0.3, 0.6, 0.9, 1.0, 1.2, 1.5, 1.8, 2.0\}$, and hardening stiffness assuming the following percentage values with respect to the initial (elastic) one $\alpha_h = \{0.0, 0.5, 1.0, 2.0, 3.0, 4.0, 5.0, 10.0\}$. Setting the elastic stiffness and the period of natural vibration, the mass of the system for each single case was consequently computed. A viscous damping ratio $\xi = 5.0\%$ was used and kept constant throughout the time-history analyses.

The analyses were performed in order to study the variation of the backbone-defining parameters, following seismic damage. Large inelastic deformations during strong ground shaking leads SDOF systems with modified IMK hysteretic model to have residual displacements and elongation of natural vibration periods. The residual displacement at a certain ductility demand depends on the hysteretic characteristics of the system and it determines the remaining ductility capacity of the post-mainshock structure. The period elongation is caused by the reduction of the peak-oriented reloading stiffness which evolves according to the modified IMK hysteretic model reported in Figure 1b. Therefore, the structure from the natural vibration period T , in intact conditions, reaches by effect of the mainshock an elongated period T_{elon}. This elongated period is calculated from the post-shock reloading stiffness at the end of the dynamic analysis, k_{ps} as $T_{elon} = 2 \cdot \pi \cdot \sqrt{m/k_{ps}}$. Figure 2 shows the effects of seismic damage on the structural backbone for an analyzed case, where k_{ps} is evident from the slope of the pushover at the end of the excitation . In particular, Figure 2a shows the initial and post-mainshock backbones of a single SDOF system, highlighting the residual displacement and the elastic stiffness variation of the SDOF structure in its post-mainshock damage state, whereas in Figure 2b, the post-mainshock-damage-state realizations of the same SDOF structure under four accelerograms of the fifty-record set are shown, revealing the record-to-record variability.

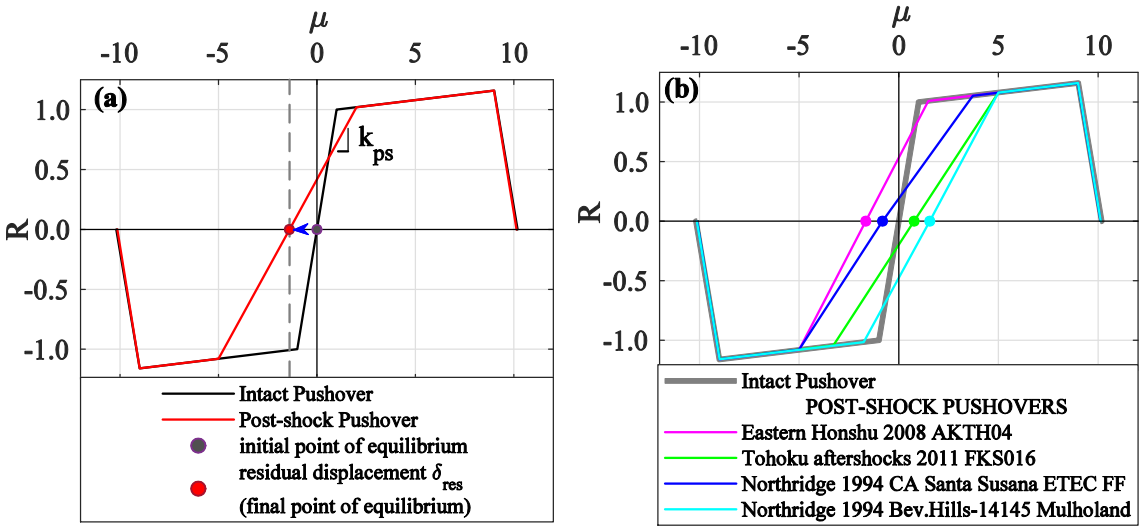

Figure 2: Examples of an SDOF structure's monotonic pushover (backbone) curve before and after the seismic damage in $\{R, \mu\}$ coordinates. Intact-structure backbone (dark line) and post-mainshock backbone (red line with pre-yield stiffness k_{ps} ,intersecting the zero-force horizontal axis at δ_{res}) for a generic analyzed case (**a**); post-mainshock backbones and residual displacements of an SDOF system with $T = 1.0s$ and $\alpha_h = 2.0\%$, evaluated for four different records scaled to cause ductility demand $\mu = 5.0$ (**b**).

3. PREDICTIVE MODEL FOR THE RESIDUAL DISPLACEMENT

During the investigation a total of 28800 elongated periods T_{elon} and constant-ductility residual displacement ratios C_μ were computed for peak-oriented bilinear systems, corresponding to fifty acceleration time histories, eight periods of natural vibration, nine levels of ductility demand and eight post-yield hardening ratios, and then processed to obtain the

predictive model. The highest C_μ value encountered among these results was 0.52. In subsequent elaborations, it was found useful to express these results in terms of the relation between the ratio of residual to peak transient displacement $\delta_{res}/\delta_{\max}$ (preserving the sign of both δ_{res} and $\delta_{\max}$ so that the ratio becomes negative when the two are in opposite directions) and $\ln(\Delta T/T)$, where $\Delta T = T_{elon} - T$ denotes the difference between the elongated post-mainshock period and the initial period. It was observed that $\delta_{res}/\delta_{\max}$ exhibits persistently high negative linear correlation with $\ln(\Delta T/T)$ for varying T, μ and α_h. In particular, values of the correlation coefficient between $\ln(\Delta T/T)$ and $\delta_{res}/\delta_{\max}$, ρ (see for example [20]), range from -0.50 to -0.99 with $\rho \le -0.7$ for the majority of analyzed cases (with $-0.5 < \rho < -0.7$ only in a few cases characterized by high ductility demands, $\mu \ge 7.0$, and long periods of natural vibration, $T \ge 1.8s$).

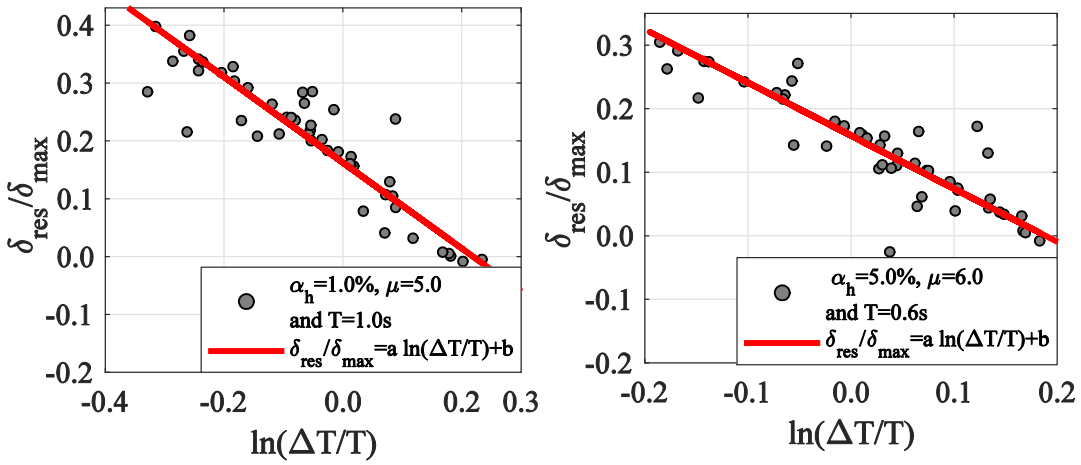

Figure 3: Examples of regression of $\delta_{res}/\delta_{\max}$ against $\ln(\Delta T/T)$ highlighting their (negative) linear correlation. Case of SDOF system with $\alpha_h = 1.0\%$, $T = 1.0s$ and $\mu = 5.0$ (left); case of SDOF system with $\alpha_h = 5.0\%$, $T = 0.6s$ and $\mu = 6.0$ (right).

This linear trend, examples of which are shown in Figure 3, motivates the adoption of a linear model for C_μ, whose slope and intercept are functions of the ductility demand μ and the post-yield hardening ratio α_h. The proposed model is given by Equation (1):

$$C_\mu = \left| \left[\beta_1 + \beta_2 \cdot (\mu - 1) + \beta_3 \cdot (\alpha_h + 1) \cdot (\mu - 1)^2 \right] \cdot \ln\left(\frac{\Delta T}{T} \right) + (\beta_4 + \beta_5 \cdot \alpha_h) \cdot (\mu - 1) + \beta_6 + \varepsilon \cdot \sigma_{C_\mu} \right| \quad (1)$$

where ε is the standard Normal variable and the parameters β_i, $i = \{1,2,...,6\}$ are coefficients estimated by means of robust regression of $\delta_{res}/\delta_{\max}$ against $\ln(\Delta T/T)$, μ, α_h using iteratively re-weighted least squares with bisquare weighting [20]. The standard deviation of the regression residual, σ_{C_μ}, was found to be non-constant, varying with T, μ and α_h (yet the residual can be assumed homoscedastic with $\ln(\Delta T/T)$ conditional on fixed values of the other independent

variables). Thus, σ_{C_μ} was also modelled analytically to account for this dependence (to follow). It should be mentioned that despite the perceived dependence of σ_{C_μ} on the oscillator's initial vibration period T, such dependence was not included in the expectation function of C_μ. In fact, according to the executed F-test [20] the null hypothesis that the slope of an additional linear term of T is zero, could not be rejected at the 5% significance level. Table 1 provides the parameter estimates for β_i appearing in Equation (1).

β_1	β_2	β_3	β_4	β_5	β_6
-0.1124	-0.1867	0.0094	0.1308	-0.6385	-0.3361

Table 1. Coefficient estimates in Equation (1).

Figure 4 shows the model for the mean of the constant-ductility residual displacement ratio for the cases with post-yield hardening ratio equal to 0.0% and 10.0%.

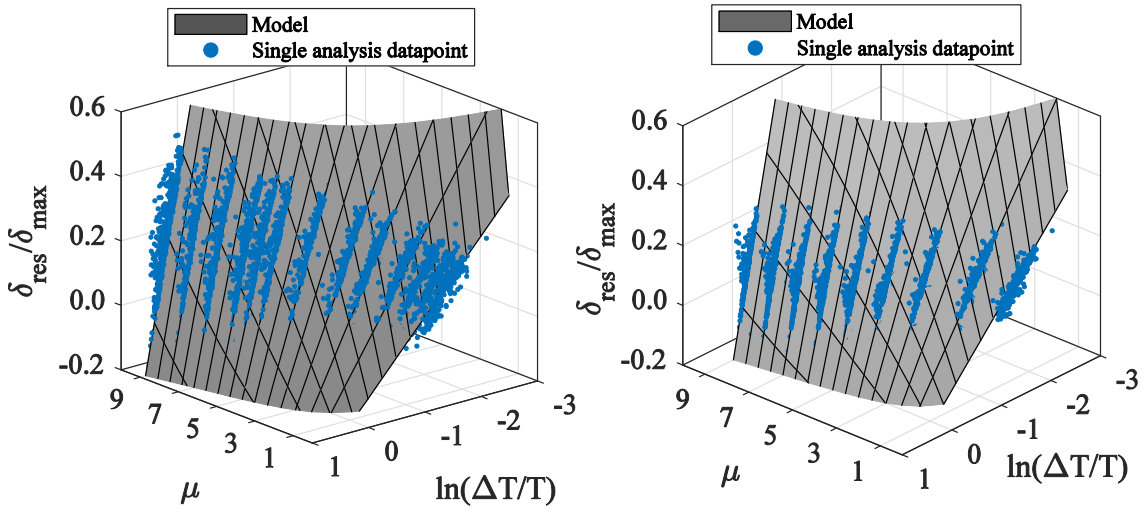

Figure 4: Central tendency of the model for the residual displacements. Case with $\alpha_h = 0.0\%$ (left); case with $\alpha_h = 10.0\%$ (right).

As already mentioned, non-constant variance of the residuals was dealt with by modelling σ_{C_μ} by means of least-squares curve-fitting of an analytical expression, with parameters γ_i, $i = \{1,2,...,7\}$, to the regression residuals for the various T, μ and α_h values, given in Equation (2):

$$\sigma_{C_\mu} = \begin{cases} \gamma_1 \cdot (\mu - 1) + \gamma_2 \cdot T \text{ , when } \alpha_h = 0 \\ \gamma_3 \cdot (\alpha_h + 1) \cdot (\mu - 1) + \gamma_4 \cdot T + \gamma_5 \cdot (\mu - 1)^2 + \gamma_6 \cdot (\mu - 1) \cdot T \cdot \alpha_h + \gamma_7 \cdot \alpha_h \text{ , when } \alpha_h > 0 \end{cases} \quad (2)$$

Due to the peculiar nature of increased response dispersion, as the post-yield stiffness of the systems goes to zero (due to the drifting effect observed for elastoplastic oscillators; e.g., [21]), Equation (2) provides separate equations for σ_{C_μ} in case of $\alpha_h = 0$ and $\alpha_h > 0$. Table 2 provides the fitted parameter values of γ_i for Equation (2).

γ_1	γ_2	γ_3	γ_4	γ_5	γ_6	γ_7
0.0090	0.0182	0.0402	0.0080	-0.0035	0.0535	0.4413

Table 2. Coefficient estimates of σ_{C_μ} in Equation (2).

Figure 5 shows the two model of standard deviation σ_{C_μ} in case of post-yield hardening ratio equal to 0.0% in Figure 5a and equal to 3.0 % in Figure 5b.

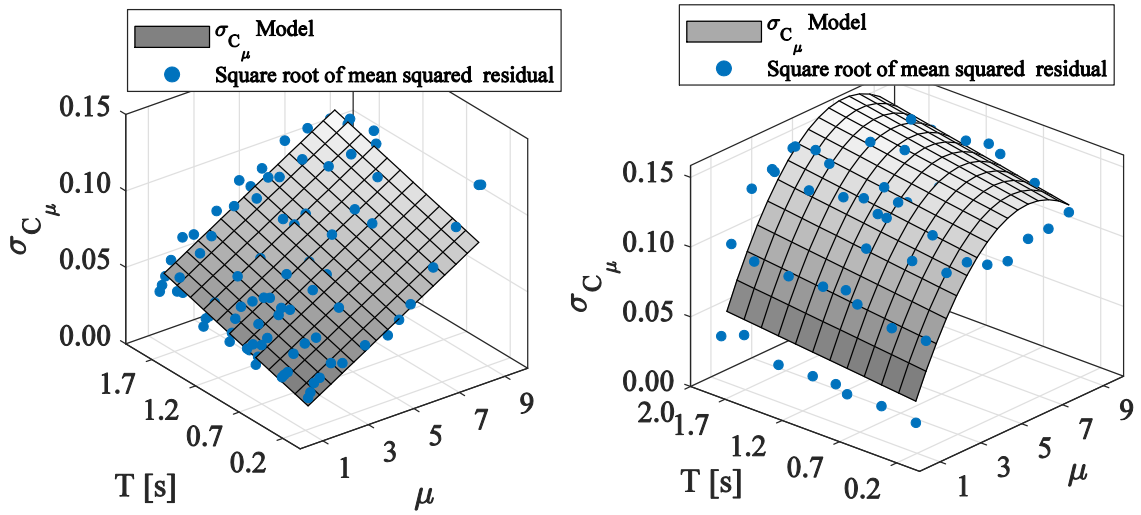

Figure 5: Models of standard deviation σ_{C_μ}. Case with $\alpha_h = 0.0\%$ (left); case with $\alpha_h = 3.0\%$ (right).

4. REGRESSION MODEL FOR PERIOD ELONGATION

The regression model for mean constant-ductility residual displacement ratios, given by Equation (1), is conditional on $\ln(\Delta T/T)$, which is also a random variable due to record-to-record variability. However, the results indicate that, given μ, α_h and T, $\ln(\Delta T/T)$ is conditionally independent of C_μ. Thus, in order to complete the predictive equation for residual displacements, an additional separate model for period elongation is needed to provide the conditional distribution of $\ln(\Delta T/T)$. The model for period elongation provides the period of the damaged structure T_{elon} at a fixed damage state represented by μ, given initial characteristics of the structure T and α_h. The analyses results were studied plotting in log-space the $\Delta T/T$ versus the ductility demand $(\mu-1)$, and assessing the dependence on independent variables T and α_h. The data showed a linear trend in log-space to each pair of T and α_h, therefore the model was realized fitting a straight line by ordinary least squares regression. The central tendency of $(\Delta T/T)$ resulted independent of the period of natural vibration T itself, whereas was strongly dependent on the post-yield hardening ratios α_h. Thus, the regression model proposed for period elongation uses only α_h and μ as predictor variables. A linear model was assumed, as reported in the following equation:

$$\ln\left(\frac{\Delta T}{T}\right)=\left(\theta_1\cdot\alpha_h+\theta_2\right)\cdot\ln\left(\mu-1\right)+\theta_3\cdot\alpha_h+\theta_4+\varepsilon\cdot\sigma_{\ln(\Delta T/T)}\ , \tag{3}$$

where ε was already defined as the standard Normal variable and $\sigma_{\ln(\Delta T/T)}$ represents the standard deviation of the regression residual, which was, also in this case, non-constant. It should be noted that, despite the Gaussian assumption for ε, for this type of hysteretic model and given μ and α_h, $\Delta T/T$ cannot exceed the value $\left(\Delta T/T\right)_{\max}$ given by Equation (4):

$$\left(\frac{\Delta T}{T}\right)_{\max}=\sqrt{\frac{2\mu-1+\alpha_h\cdot\left(\mu-1\right)}{1+\alpha_h\cdot\left(\mu-1\right)}}-1 \tag{4}$$

As reported in Equation (3), the slope and the intercept of the model for period elongation are only dependent on α_h. The coefficients $\theta_i, i=\{1,2,3,4\}$, were evaluated by curve fitting of the single regressions results performed for each value of α_h. A weighted regression, on account of the non-constant variance, was not deemed necessary because the ratio of the maximum to the minimum value of the mean squared error of the residuals did not exceed 1.5, as suggested in [15]. In Table 3 the values of the coefficients which characterize Equation (3) are reported.

θ_1	θ_2	θ_3	θ_4
-0.906	0.867	-1.163	-1.276

Table 3. Coefficient estimates of Equation (3).

Figure 6 shows the model fitted against the analysis results of SDOFs with α_h equal to 1.0% and T varying in the entire range considered, as well as a 3D graph of the model for period elongation, highlighting the dependence of its central tendency on α_h and μ.

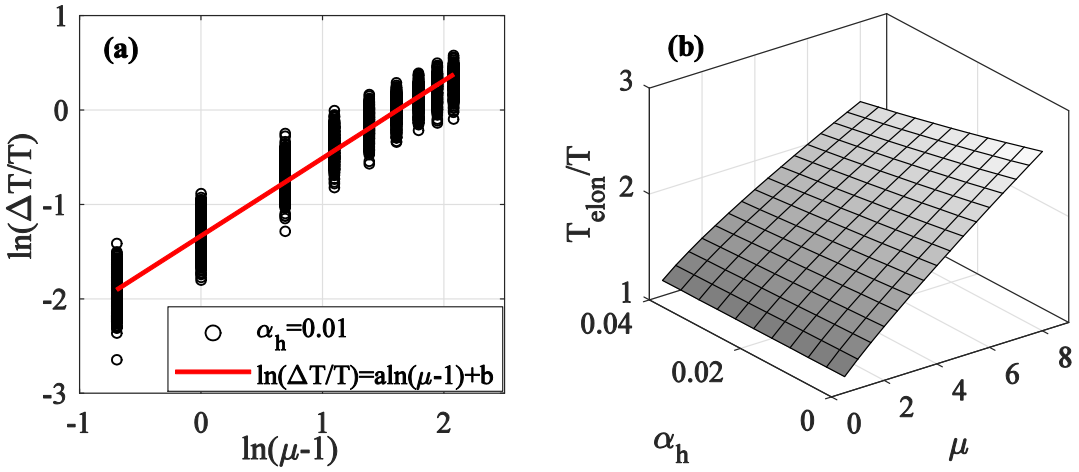

Figure 6: Central tendency of model for period elongation. Regression example of the form $\ln\left(\Delta T/T\right)=a\cdot\ln(\mu-1)+b$ used to define the model for period elongation evaluated in the case of post-yield hardening ratios α_h equal to 1.0% (**a**); Model for period elongation (**b**).

Finally, an analytical expression was proposed, to express the dependence of $\sigma_{\ln(\Delta T/T)}$ with the intact structure's period T and the hardening slope α_h, given by Equation (5) :

$$\sigma_{\ln(\Delta T/T)} = \xi_1 \cdot T + \xi_2 + \xi_3 \cdot \alpha_h + \xi_4 \cdot T^2 \tag{5}$$

Table 4 provides the values of the parameters ξ_i, $i = \{1,2,3,4\}$, appearing in Equation (5), estimated from curve-fitting against the regression residuals.

ξ_1	ξ_2	ξ_3	ξ_4
0.0472	0.1444	-0.1993	-0.0151

Table 4. Coefficient estimates for Equation (5).

Figure 7 shows the model of the standard deviation $\sigma_{\ln(\Delta T/T)}$ as a function of the hardening slope α_h and the period of natural vibration T.

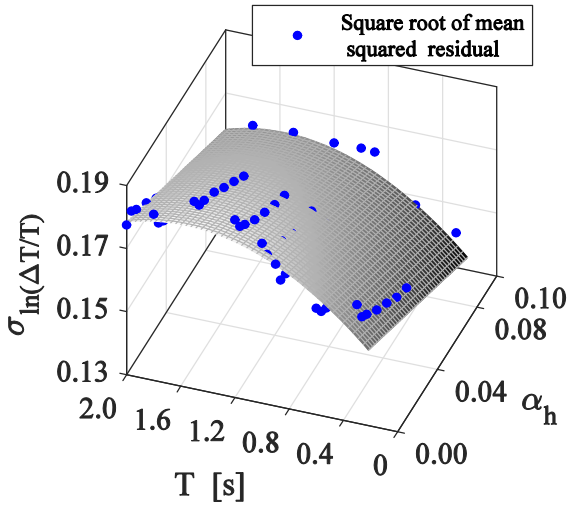

Figure 7: Model of standard deviation $\sigma_{\ln(\Delta T/T)}$.

5. PUTTING THE TWO COMPONENTS OF THE MODEL TOGETHER

Having completely defined both models, for period elongation and residual displacement, and recalling that period elongation was found conditionally independent of the residual displacement, it is possible to estimate the joint conditional distribution of the two random variables, given the ductility demand μ, the period T and the hardening slope α_h of the initial structure. Due to the fact that in Equation (1) C_μ is given by the absolute value of a regression model for $\delta_{res}/\delta_{\max}$, it is convenient to visualize its conditional joint distribution with relative period elongation T_{elon}/T by means of a Monte-Carlo sampling scheme. This entails fixing the values of T, α_h and μ, calculating the mean and standard deviation of $\ln(\Delta T/T)$ conditional to these values from Equations (3) and (5) and then extracting a random sample of $\ln(\Delta T/T)$ values from a normal distribution with that mean and $\sigma_{\ln(\Delta T/T)}$, truncated according to Equation

(4). Subsequently, the conditional mean and standard deviation of the ratio $\delta_{res}/\delta_{\max}$ is obtained for each sampled value of $\ln(\Delta T/T)$, from Equations (1) and (2), and a $\delta_{res}/\delta_{\max}$ value is randomly sampled from the corresponding normal distribution, truncated between -1 and 1. This amounts to random sampling of $\{\ln(\Delta T/T), \delta_{res}/\delta_{\max}\}$ from their joint conditional distribution. Finally, C_μ values are obtained by taking the absolute value of $\delta_{res}/\delta_{\max}$. An example of such a representation is reported in Figure 8a, that was constructed by sampling one thousand value-pairs from the joint distribution of $\delta_{res}/\delta_{\max}$ and $\ln(\Delta T/T)$. A representation of the marginal density of C_μ and its mean is also reported in Figure 8b, estimated during the same procedure.

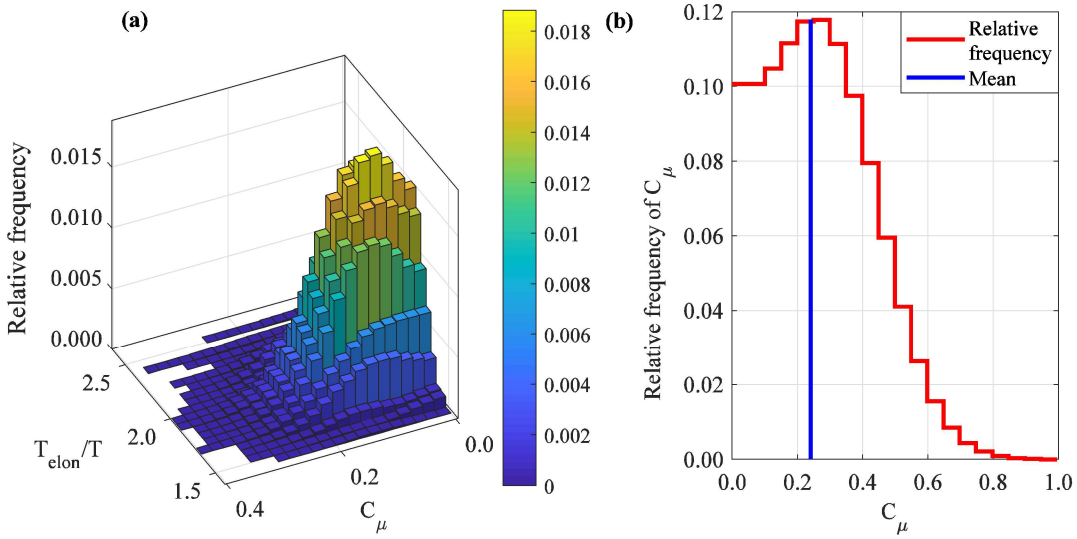

Figure 8. Sampling-based representation of the joint relative frequency of period elongation and residual displacement ratio (**a**), relative frequency of C_μ (**b**), for the case of ductility demand $\mu = 5.0$, post-yield hardening ratio $\alpha_h = 2.0\%$ and period of the initial structure $T = 0.9s$.

6. MODEL VALIDATION

To validate the predictive model a set of analyses for blind-testing the goodness-of-fit was performed. These analyses were organized in three groups: the first group was executed fixing the mass of SDOF systems and varying the elastic stiffness to achieve the required periods of natural vibration, whilst the analyses performed for the model evaluation, fixed the elastic stiffness and varied the mass to the same effect. The second group of analyses was executed levels of ductility demand and values of post-yield hardening ratio different from the ones used for fitting development the predictive model. The last group was performed using a different set of fifty records for IDA. To evaluate the accuracy of the predictive models in estimating elongated periods and residual displacements, the root mean square error (RMSE [20]) was computed for each group of analyses, according to Equation (6) .

$$RMSE = \sqrt{\frac{\sum_{i=1}^{n}(y_i - \bar{y})^2}{n}} \qquad (6),$$

where $\bar{y}$ is the generic model of either $\ln(\Delta T/T)$ or C_μ, y_i is the data point from the i-th analysis and n is the total number of analyses run.

These RMSE values were employed to assess the goodness-of-fit for Equations (1),(3) in estimating mean C_μ and $\ln(\Delta T/T)$. In detail, the root mean square error measure was computed for the three groups of test data, comparing the results with the error evaluated on the entire data set used for fitting development the predictive model. Table 5 provides $RMSE_{\ln(\Delta T/T)}$ for the first and the second group of analyses defined by different values of μ and T.

Constant mass				Independent variable values (α_h, μ) not used in fitting the model			
T	μ	α_h	$RMSE_{\ln(\Delta T/T)}$	T	μ	α_h	$RMSE_{\ln(\Delta T/T)}$
0.3	4.0	0.02	0.024	0.3	4.3	0.07	0.020
0.6	4.0	0.02	0.016	0.6	4.3	0.07	0.013
2.00	4.0	0.02	0.008	2.00	4.3	0.07	0.002

Table 5. Values of $RMSE_{\ln(\Delta T/T)}$ for the first and the second group of validation analyses.

Table 6. provides $RMSE_{\ln(\Delta T/T)}$ for the third group of analyses executed fixing the ductility demand, the hardening slope and employing a new set of fifty acceleration records recorded on firm soil or rock and devoid of apparent directivity effects.

Using a different set of records			
T	μ	α_h	$RMSE_{\ln(\Delta T/T)}$
0.3	5.0	0.04	0.010
0.6	5.0	0.04	0.003
2.00	5.0	0.04	0.016
0.3	8.0	0.05	0.048
0.6	8.0	0.05	0.002
2.00	8.0	0.05	0.006

Table 6. Values of $RMSE_{\ln(\Delta T/T)}$ for the third group of validation analyses.

The values of $RMSE_{\ln(\Delta T/T)}$ previously reported are very close to the value evaluated on the data set used for fitting development the predictive model which is 0.024.

To evaluate the accuracy of the predictive model in estimating residual displacement, the error measure RMSE was computed for the three groups of test data. In particular, it was evaluated for C_μ as provided by the Equation (6). The values of RMSE for the three group of analyses are reported in Table 7 and Table 8. The values of $RMSE_{C_\mu}$ previously reported are very close to the value estimated on the data set used for fitting development the predictive model which is 0.056.

Constant mass				Independent variable values (α_h, μ) not used in fitting the model			
T	μ	α_h	$RMSE_{C_\mu}$	T	μ	α_h	$RMSE_{C_\mu}$
0.3	4.0	0.02	0.029	0.3	4.3	0.07	0.025
0.6	4.0	0.02	0.040	0.6	4.3	0.07	0.030
2.00	4.0	0.02	0.065	2.00	4.3	0.07	0.077

Table 7. Values of $RMSE_{C_\mu}$ for the first and second group of validation analyses.

Using a different set of records			
T	μ	α_h	$RMSE_{C_\mu}$
0.3	5.0	0.04	0.063
0.6	5.0	0.04	0.045
2.00	5.0	0.04	0.050
0.3	8.0	0.05	0.085
0.6	8.0	0.05	0.065
2.00	8.0	0.05	0.087

Table 8. Values of $RMSE_{C_\mu}$ for the third group of validation analyses.

7. DISCUSSION AND CONCLUSIONS

The main purpose of this study was to present a predictive model for the central tendency and related record-to-record variability of residual displacements for bilinear single-degree-of-freedom systems (SDOF). To this end, a probabilistic model for the constant-ductility residual displacement ratio, C_μ, was introduced. The residual displacement ratio, defined as the absolute-value ratio of residual to peak transient displacement, was calculated for various combinations of input motion, natural vibration period and post-yielding hardening ratio, via nonlinear dynamic analysis designed to hold the ductility demand μ constant, by appropriately scaling the input motion. Thus, SDOF systems with non-degrading, peak-oriented hysteretic response, according to the modified *Ibarra-Medina-Krawinkler* model, were analyzed subjected to a set of fifty earthquake ground motions recorded on firm site conditions. From the data obtained during the dynamic analyses, it was observed that the residual displacement demand did not exceed 52% of the peak inelastic displacement demand and is mainly affected on post-yield hardening ratio. In fact, the SDOF systems with higher post-yield stiffness ratio exhibit smaller residual displacement ratios on average, in agreement with previous studies.

The two-part predictive model was derived via two-stage regression: the first-stage regression model provides a prediction for the post-shock elongated period and the second one accounts for the residual displacement of the system conditional to its elongated period. It was found that central tendency of constant-ductility residual displacement ratios depends on the ductility demand, the post-yield hardening ratio and ratio of post-shock elongated period to the initial period of natural vibration, while the non-constant variance of the residual displacement ratio mainly depends on the post-yield hardening slope of the structure in its initial (undamaged) condition. It was also found that the period elongation has a central tendency that only depends on post-yield hardening ratio and ductility demand, whereas the corresponding variance also exhibits some dependence on the structural period of natural vibration. Finally, it should be mentioned that the complete model proposed, allows to estimate the joint conditional

distribution of the two random variables: residual displacement and period elongation, given ductility, period and hardening slope.

ACKNOWLEDGEMENTS

The work presented in this paper was developed within the activities of ReLUIS (*Rete di Laboratori Universitari di Ingegneria Sismica*) during the 2014-2018 research program, financed by the Department of Civil Protection (*Dipartimento della Protezione Civile* - DPC).

REFERENCES

[1] C.A. Cornell, H. Krawinkler, Progress and Challenges in Seismic Performance Assessment. *PEER Center News*, **3**, 1–4, 2000.

[2] P. Bazzurro, C.A. Cornell, C. Menun, M. Motahari, Guidelines for seismic assessment of damaged buildings. *Proceedings of the 13th World Conference on Earthquake Engineering,* Vancouver, Canada, August 1-6, 2004.

[3] N. Luco, P. Bazzurro, C. A. Cornell, Dynamic Versus Static Computation Of The Residual Capacity Of A Mainshock-damaged Building To Withstand An Aftershock. *Proceedings of the 13th World Conference on Earthquake Engineering,* Vancouver, Canada, August 1-6, 2004.

[4] J. Ruiz-García, E. Miranda, Residual displacement ratios for assessment of existing structures. *Earthquake Engineering and Structural Dynamics*, **35**, 315–336, 2006.

[5] S. Mahin, V. V. Bertero, An Evaluation of Inelatic Seismic Design Spectra. *Journal of Structural Engineering (ASCE)*, **107**, 1777–1795, 1981.

[6] G.A. Macrae, K. Kawashima, Post-earthquake residual displacements of bilinear oscillators. *Earthquake Engineering and Structural Dynamics*, **26**, 701–716, 1997.

[7] B.K. Kawashima, M. Asce, G.A. Macrae, Residual displacement response spectrum. *Journal of Structural Engineering*, 523–530, 1998.

[8] B. Borzi, G. M. Calvi, A. S. Elnashai, E. Faccioli, J. J. Bommer, Inelastic spectra for displacement-based seismic design. *Soil Dynamics and Earthquake Engineering*, **21**, 47–61, 2001.

[9] S. Pampanin, C. Christopoulos, M.J. Nigel Priestley, Performance-based seismic response of frame structures including residual deformations. Part II: Multi-degree of freedom systems. *Journal of Earthquake Engineering*, **7**, 119–147, 2003.

[10] J. Ruiz-García, E. Miranda, Performance-based assessment of existing structures accounting for residual dispalcements. Stanford University, Stanford, CA, 2004.

[11] E. Liossatou, M. N. Fardis, Residual displacements of RC structures as SDOF systems. *Earthquake Engineering and Structural Dynamics*, **44**, 713–734, 2015.

[12] G. Baltzopoulos, R. Baraschino, I. Iervolino, D. Vamvatsikos, SPO2FRAG: software for seismic fragility assessment based on static pushover. *Bulletin of Earthquake Engineering*, **15**, 2017.

[13] I. Iervolino, A. Spillatura, P. Bazzurro, Seismic Reliability of Code-Conforming Italian Buildings. *Journal of Earthquake Engineering*, **22,** 5-27, 2018.

[14] M. Raghunandan, A. Liel, N. Luco, Aftershock collapse vulnerability assessment of reinforced concrete frame structures. *Earthquake Engineering and Structural Dynamics*, **44**, 419–439, 2015.

[15] T. P. Ryan, *Modern Regression Methods, 2th Edition*. A. John Wiley & Sons,1945.

[16] L. F. Ibarra, R. A. Medina, H. Krawinkler, Hysteretic models that incorporate strength and stiffness deterioration. *Earthquake Engineering and Structural Dynamics*, **34**, 1489–1511, 2005.

[17] D. Lignos, Sidesway collapse of deteriorating structural systems under seismic excitations. *PhD Thesis*, **53**,1689–1699, 2013.
[18] D. Vamvatsikos, C. Allin Cornell, Incremental dynamic analysis. *Earthquake Engineering and Structural Dynamics*, **31**, 491–514, 2002.
[19] F. Pacor, C. Felicetta, G. Lanzano, S. Sgobba, R. Puglia, M. D'Amico, *et al.*, NESS v1.0: A worldwide collection of strong-motion data to investigate near source effects. *Seismological Research Letters*, 2018.
[20] N. R. Draper, H. Smith, *Applied regression analysis*, *3th Edition*. New York. John Wiley & Sons, 1998.
[21] R. Bouc, D. Boussaa, Drifting response of hysteretic oscillators to stochastic excitation , **37**, 1397–1406, 2002.